

NATIONAL EARTHQUAKE HAZARDS REDUCTION PROGRAM
FINAL TECHNICAL REPORT
JUNE 11, 2020

Grant Number: G19AP00053 and G19AP00054

Project Title: Quantifying the geologic and geodetic distribution and transfer of slip rate on the southern San Andreas fault from the northern Coachella Valley to the Eastern California Shear Zone across the Eastern Transverse Ranges: Collaborative Research between San Jose State University and University of Arizona

Project Start Date: June 1, 2019

Principle Investigator (UA): Richard Bennett
Department of Geosciences
University of Arizona
Gould-Simpson Building, 1040 E 4th Street
Tucson, AZ. 85721
Phone: (520) 621-6000

Co-Investigator (SJSU): Kimberly Blisniuk
San Jose State University
Department of Geology
One Washington Square, Duncan Hall Room 222
San Jose, CA 95192-0201
Phone: (408) 924-5045

NON-TECHNICAL SUMMARY

Figuring out how strain is accumulating along faults near the geometrically complex area of San Geronimo Pass, California is critical for evaluating which particular faults may play a larger role in accommodating plate boundary motion, and importantly which faults may be more likely to produce large-magnitude earthquakes. The region of the Eastern Transverse Ranges (ETR) rests directly in between two larger tectonic provinces: the Southern San Andreas Fault (SSAF) and the Eastern California Shear Zone (ECSZ), and therefore may serve as a transfer zone between the two systems. Moreover, the ETR province includes many different fault systems that have had varying activity levels and lifetimes in most recent geologic history, including the N-S trending faults in the Little San Bernardino Mountains and the E-W trending faults of the ETR system. Determining which of these many faults is most active in the modern day will allow us to better understand what mechanisms of transfer could explain the occurrence of multiple large magnitude earthquakes in the ECSZ over the last three decades, with important implications also for the earthquake potential of the SSAF.

In this project we have endeavored to increase our understanding of the pattern of strain transfer between the SSAF and the ECSZ by applying tectonic geomorphology and tectonic geodesy to discriminate between two competing hypotheses about where strain is being accumulated in the ETR region. On one hand, strain may be directly transferred between the SSAF and ECSZ along the apparently emergent N-S trending Eureka Peak fault system. On the other hand, strain could be transferred by block rotation of Eastern Transverse Ranges blocks facilitated by left lateral slip on the Blue Cut, Pinto Mountain, and potentially other transverse faults.

We document in this report how we have been able to (1) quantify the late Quaternary slip history of the Blue Cut Fault, a fault whose activity is required to permit block rotation to occur, (2) process and update a new Global Positioning System (GPS) velocity field for southern California using new collected campaign data, (3) remove modeled viscoelastic postseismic displacements from this updated velocity field to produce a “postseismic-reduced” velocity field, and (4) synthesize both geologic and geodetic datasets in a suite of elastic fault block models to test geometry hypotheses about the area to see which fault geometries fit the different datasets best.

RESULTS

(1) Quantifying the late Quaternary record of slip along the Blue Cut Fault, G19AP00054

Through tectonic geomorphologic mapping and ^{10}Be Cosmogenic Radionuclide surface exposure dating, we have explored and measured the late Pleistocene and possibly earliest Holocene displacements along the Hexie Mountains section of the Blue Cut Fault to estimate its slip rate. We document offsets from five different age left-laterally offset alluvial surfaces near the Cholla Gardens of Joshua Tree National Park. Our 27 current ^{10}Be ages sampled from boulder tops, cobbles and amalgamated pebble samples indicate a spread of ages as old as 133 ka and as young as 10.6 ka. Qf1a is our oldest preserved surface that has been offset, while our youngest offset surface is bracketed as younger than 10.6 ka, but older than our youngest undeformed surface. We use the four best-constrained surface offsets and surface ages to calculate an overall late-Pleistocene slip rate of 1.66 ± 0.44 (± 2 sigma) across our two neighboring sites. When we look at individual surface slip rates over time, the results suggest that the Blue Cut slip rate is decreasing along the Hexie Mountains strand, with slip rates >2.2 mm/yr before 100 ka and rates <1.2 mm/yr after 70 ka. If the Blue Cut Fault is slowing down, as indicated by our preliminary results, this could suggest that the hypothesis of block rotation as a mechanism of strain transfer may not be the most important mechanism in this system, and that another system may be taking over.

(2) *Collecting and Incorporating New Campaign GPS Data*, G19AP00053

Over the years 2016 to 2018 we collected 6 surveys worth of campaign GPS data within Joshua Tree National Park. These campaign stations are part of the Joshua Tree Integrative Geodetic Network (JOIGN), which is monitored by the University of Arizona. We processed this campaign data to calculate a new GPS velocity field for southern California. In addition, we incorporated two years-worth of campaign GPS data from the San Bernardino Mountains collected by Sally McGill and her group at California State University, San Bernardino. Incorporating this campaign data allows us to increase the resolution of velocity points in our

deformation field, particularly in areas of large expanses of wilderness, such as the highlands of Joshua Tree National Park, and the rugged San Bernardino Mountains.

(3) Removing Ongoing Viscoelastic Postseismic Displacements from the Deformation Field, G19AP00053

High precision GPS time series measures both long- and short-term signals caused by everything from volcanic activity, to anthropogenic activities, to seasonal water storage, to post-earthquake process. In order to produce a time-invariant GPS time series dataset, we remove observed and conspicuous seasonal and postseismic signals, and then take another step further and account for measurable ongoing postseismic transients from historical and recent large-magnitude earthquakes in southern California. We forward model the viscoelastic postseismic displacements for all $\geq M_{\text{w}}6.0$ earthquakes that have occurred since year 1800 using a laterally homogenous chosen viscoelastic Earth model structure. We find that 12 of these earthquakes produce ≥ 0.35 mm of postseismic displacement in the modern-day observation period, which is measurable with high-precision continuous GPS instruments. These earthquakes include, in time-order, the 1812 $M_{\text{w}}7.5$ Wrightwood, 1857 $M_{\text{w}}7.9$ Fort Tejon, 1872 $M_{\text{w}}7.4$ Lone Pine/Owens Valley, 1892 $M_{\text{w}}7.3$ Laguna Salada, 1906 $M_{\text{w}}7.8$ San Francisco, 1918 $M_{\text{w}}6.8$ San Jacinto, 1952 $M_{\text{w}}7.5$ Kern County, 1992 $M_{\text{w}}7.3$ Landers, 1994 $M_{\text{w}}6.7$ Northridge, 1999 $M_{\text{w}}7.1$ Hector Mine, 2010 $M_{\text{w}}7.2$ El Mayor-Cucapah, and the 2012 $M_{\text{w}}7.0$ Baja California events (**Figure 1**).

Once we identified which earthquakes produced measurable viscoelastic postseismic displacements, we subtract the modeled co- and postseismic displacements from our observed coordinate time series to produce a postseismic-reduced time series dataset. To remove any further leftover postseismic displacements, we estimate a single logarithmic amplitude term for earthquake events that have occurred during the GPS observation period. When we do this step for both our observed and our postseismic-reduced datasets, we compare the two for the 2010 El Mayor-Cucapah earthquake and find that our forward modeling step reduced postseismic by up to 60% for this event.

Removing postseismic deformation in this way allows us to estimate velocities that better approximate the long-term deformation field. In addition, with this newly created dataset, we can not only estimate geodetic fault slip rates that are not impacted by postseismic transients, but we can also quantify the effects that postseismic transients have on estimated fault slip rates in southern California.

The methodology and results of this analysis are now published as Guns & Bennett (2020) in the Journal of Geophysical Research: Solid Earth.

(4) Synthesizing Geologic and Geodetic Results into Elastic Fault Block Models, G19AP00053 and G19AP00054

With this new postseismic-reduced GPS dataset, and a compiled catalog of geologic slip rates in southern California (in addition to our newly constrained geologic slip rate along the Blue Cut Fault), we create a suite of sixteen elastic fault block models to evaluate what fault geometry in the area of San Geronio Pass best fits the modern day GPS data and which fits the longer-term geologic data. This suite of block models allows us to additionally assess the questions of (1) what effect does ongoing viscoelastic postseismic deformation have on the estimated fault slip rates of southern California? (2) Does the removal of postseismic deformation help address or resolve any of the geologic-geodetic slip rate discrepancies in southern California? (3) Is this new dataset, which includes campaign data from San Geronio

Pass and the San Bernardino Mountains, able to inform how many active fault strands are needed to accommodate slip in San Gorgonio Pass? And most relevant to our mission in this project, (4) Do the outcomes of these block models favor one strain transfer mechanism over another in the ETR region?

Three model geometries best fit our different datasets (**Figure 2**): Our best fit model to the postseismic-reduced GPS dataset is our model that includes all blocks and faults except for the Galena Peak Fault (SGP2, **Figure 2A**). This same model also fits the Pleistocene-only geologic slip rates based on a RMS score we calculate. The best-fit model to the overall geologic data (including a combination of both Holocene and Pleistocene geologic slip rate estimates) is a model that includes all faults except for the Galena Peak Fault and the Blue Cut Fault in the ETR (SGP4, **Figure 2C**). Lastly, our best-fit model to the Holocene-only geologic slip rate data is a model that includes all faults except a Blue Cut Fault, a Galena Peak Fault, and a West-Pinto Mountain Fault (SGP7, **Figure 2B**).

The primary effect that postseismic deformation appears to have on our estimated fault slip rates is to increase their rates everywhere except for four fault segments. The majority of faults in our model geometry experience an increase in fault slip rate higher than their 1 sigma uncertainties. The largest change in slip rate of ~6 mm/yr lies along the Mojave segment of the SSAF, though this lies at the edge of our model domain. In San Gorgonio Pass, rates actually decrease slightly when postseismic deformation is included, indicating the possibility that postseismic deformation may have an inhibiting effect on fault motion.

With regards to the geologic-geodetic slip rate discrepancy debates in southern California, our results indicate that when we remove postseismic displacements and account for off-fault deformation in the southern Mojave, we can resolve the geologic-geodetic discrepancy there. With our best-fit model to GPS data, SGP2, we calculate a summed slip rate across the southern ECSZ of 7.2 ± 2.8 mm/yr when we account for off-fault deformation as recommended by Herbert et al. (2014). This summed slip rate fits directly in the range of observed geologic slip rates in the region. On the other hand, discrepancies along the Mojave and San Bernardino segments of the SSAF system are amplified by our postseismic reductions, indicating that there is more to investigate here.

When we turn our attention to the fault strands running through the San Gorgonio Pass area, our results suggest that two strands of the SSAF here are necessary to keep slip rates sufficiently low as to match the geologic slip rate observations along the San Gorgonio Pass Thrust and Banning faults. There has been much recent debate about the activity of the Mission-Mill Creek Fault in San Gorgonio Pass, and we attempted to probe our dataset to distinguish between models that include one fault running through the pass (the Banning-San Gorgonio Pass Thrust Fault), and models that include two (or more) strands (including the Banning-San Gorgonio Pass Thrust and the Mission-Mill Creek, and/or the Galena Peak strand). Our best-fitting model to GPS data (**Figure 2A**) indicates that a Banning-San Gorgonio Pass Thrust fault and a Mission-Mill Creek fault are needed; however, this model only allows for 0.1 – 1.8 mm/yr of slip along the Mission-Mill Creek which could be consistent with observation that the Mission-Mill Creek Fault is not very active (if active at all). The model that produces slip rates along the San Gorgonio Pass Thrust that best match geologic slip rates there is model SGP7, which is our model that best fits Holocene geologic rates (**Figure 2B**). This model has two strands in San Gorgonio Pass, and while the southern strand fits geologic observations well, the northern strand exhibits estimated rates of 4.5 – 4.8 mm/yr, which may be higher than what has been observed along the Mission-Mill Creek fault.

Lastly, to answer the question of how strain may be transferring between the SSAF and the ECSZ, we tested several different model geometries that included a Eureka Peak Fault/Mojave Seismic Line alone, block rotation faults alone (no Eureka Peak fault), and combinations of both geometries. When we look only to the geodetic data, the top three best-fit models to GPS data all include a combination of Eureka Peak fault and block rotation faults. On the other hand, when we look through the perspective of the geologic slip rate data, Pleistocene slip rate data is best fit by a model that includes a combination, while more recent Holocene geologic slip rate data is best fit by a model that does not include two block rotation faults: the West Pinto Mountain Fault and the Blue Cut Fault. While this is not conclusive in and of itself, given that block models can have nearly equally low misfit values for different geometries, when taken with the geologic slip rate evidence that the Blue Cut Fault might be slowing down over the Late Pleistocene and earliest Holocene, this may be an indication that block rotation may not be the most important mechanism of strain transfer, despite it having been occurring for millions of years.

The methodology and results of our elastic fault block modeling is currently in revision and review with the journal of Geosphere.

PUBLICATIONS

Guns, K.A., & Bennett, R.A. (2020). Assessing long-term postseismic transients from GPS time series in Southern California. *Journal of Geophysical Research: Solid Earth*, 125(4), <https://doi.org/10.1029/2019JB018670>.

Guns, K.A., Bennett, R.A., Spinler, J.C., & McGill, S.F., in revision, New geodetic constraints on southern San Andreas Fault slip rates, San Geronio Pass, California: *Geosphere*.

Guns, K.A., Bennett, R.A., Blisniuk, K., & Walker, A., in prep, Evaluating the late Quaternary record of fault slip in the Eastern Transverse Ranges, CA: New time-variable geologic slip rates along the Blue Cut Fault: *GSA Bulletin*

Guns, K.A., & Bennett, R.A., in prep, Can ongoing viscoelastic postseismic deformation affect regional fault loading?: *Geology*

FIGURES

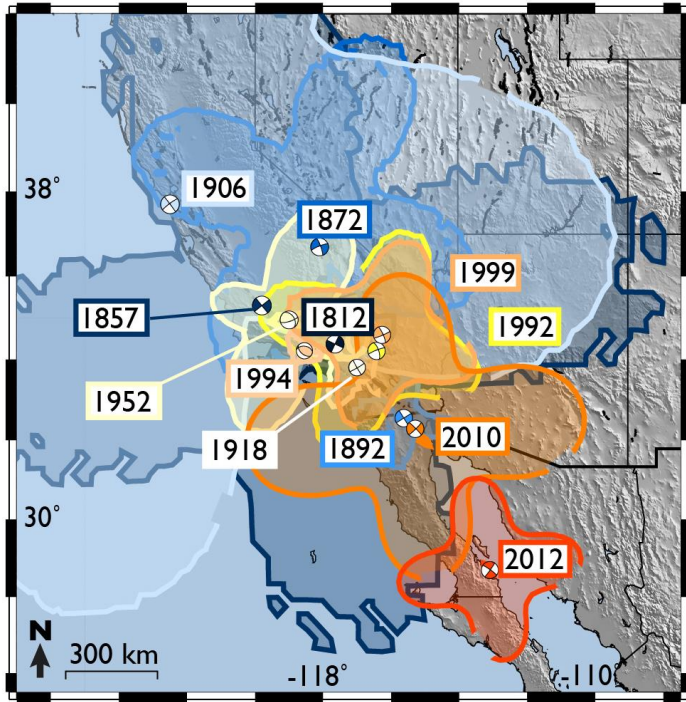


Figure 1. (Figure 5 of Guns & Bennett (2020)) Extent of measurable horizontal displacements in the year 2018 due to viscoelastic deformation following each of the 12 earthquakes that accumulate ≥ 0.35 mm in any year of our time series (2000 – 2018). Any space inside the 0.35 mm contour indicates it has larger than 0.35 mm displacements accumulated in the time span between 1 January 2018 and 1 January 2019 and is therefore measureable by GPS instruments.

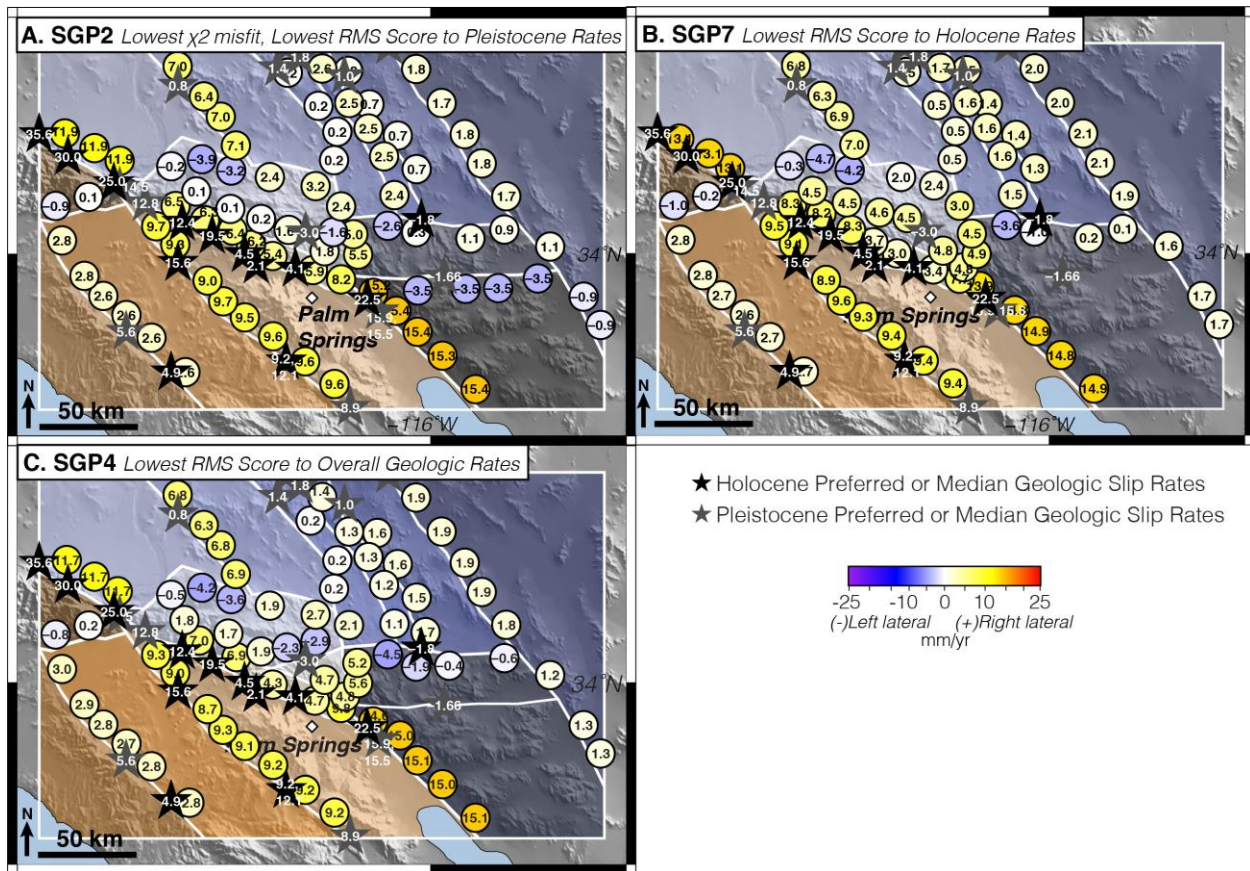


Figure 2. Our three best fitting models across different categories of fitness, with their slip rate estimates along all included fault strands; (A) SGP2 which has the lowest χ^2 misfit to GPS data and the lowest RMS score to the Late Pleistocene geologic slip rates; (B) is model SGP7 which has the lowest RMS score to the Holocene only geologic slip rates; (C) is model SGP4 which has the lowest RMS score to the Overall Geologic slip rates.